

1 **Transcriptional activity differentiates families of Marine Group II *Euryarchaeota* in the**
2 **coastal ocean**

3

4 Julian Damashek^{1,3}, Aimee O. Okotie-Oyekan^{1,4}, Scott M. Gifford², Alexey Vorobev^{1,5}, Mary
5 Ann Moran¹, James T. Hollibaugh¹

6

7 ¹Department of Marine Sciences, University of Georgia, Athens, GA, USA

8 ²Department of Marine Sciences, University of North Carolina, Chapel Hill, NC, USA

9 ³Present address: Department of Biology, Utica College, Utica, NY, USA

10 ⁴Present address: Environmental Studies Program, University of Oregon, Eugene, OR, USA

11 ⁵Present address: INSERM U932, PSL University, Institut Curie, Paris, France

12

13 Corresponding author:

14 Julian Damashek

15 Utica College

16 1600 Burrstone Road, Utica, NY 30602

17 (315) 223-2326; judamash@utica.edu

18

19 **ABSTRACT**

20 Marine Group II *Euryarchaeota* (*Candidatus* Poseidoniales) are abundant members of
21 marine microbial communities. They are thought to be (photo)heterotrophs that metabolize
22 components of dissolved organic matter (DOM) such as lipids and peptides, but little is known
23 about their transcriptional activity. We mapped reads from metatranscriptomes collected off
24 Sapelo Island, GA to metagenome-assembled genomes to determine the diversity of
25 transcriptionally-active *Ca.* Poseidoniales. Summer metatranscriptomes had the highest
26 abundance of *Ca.* Poseidoniales transcripts, mostly from the O1 and O3 genera within *Ca.*
27 *Thalassarchaeaceae* (MGIIb). In contrast, transcripts from fall and winter samples were
28 predominantly from *Ca.* Poseidoniaceae (MGIIa). Genes encoding proteorhodopsin, membrane-
29 bound pyrophosphatase, peptidase/proteases, and part of the β -oxidation pathway were highly
30 transcribed across abundant genera. Highly transcribed genes specific to *Ca.* *Thalassarchaeaceae*
31 included xanthine/uracil permease and receptors for amino acid transporters. Enrichment of *Ca.*
32 *Thalassarchaeaceae* transcript reads related to protein/peptide, nucleic acid, and amino acid
33 transport and metabolism, as well as transcript depletion during dark incubations, provided
34 further evidence of heterotrophic metabolism. Quantitative PCR analysis of South Atlantic Bight
35 samples indicated consistently abundant *Ca.* Poseidoniales in nearshore and inshore waters.
36 Together, our data suggest *Ca.* *Thalassarchaeaceae* are important photoheterotrophs potentially
37 linking DOM and nitrogen cycling in coastal waters.

38

39 INTRODUCTION

40 Since the initial discovery of Marine Group II (MGII) *Euryarchaeota* [1,2], definitive
41 determination of their physiology and ecological roles has remained challenging due to the lack
42 of a cultivated isolate. Nonetheless, as data describing MGII distributions throughout the oceans
43 have increased, several patterns have emerged: MGII are often highly abundant in the euphotic
44 zone and in coastal waters, reach high abundance following phytoplankton blooms, and are
45 largely comprised of two subclades, MGIIa and MGIIb [3,4]. Early metagenomic studies
46 provided the first evidence that MGII may be aerobic (photo)heterotrophs [5-7], a hypothesis
47 supported by incubation experiments [8-10] and by the gene content of diverse metagenome-
48 assembled genomes (MAGs) [11-14]. Two recent studies deepened our understanding of the
49 phylogenomics and metabolic potential of MGII by analyzing hundreds of MAGs, highlighting
50 clade-specific differences in genomic potential for transport and degradation of organic
51 molecules, light harvesting proteorhodopsins, and motility [15,16]. Here, we refer to MGII as the
52 putative order “*Candidatus* Poseidoniales,” MGIIa and MGIIb as the putative families “*Ca.*
53 *Poseidoniaceae*” and “*Ca. Thalassarchaeaceae*,” respectively, and putative genera as specified by
54 Rinke et al. [15]. We occasionally use “MGIIa” and “MGIIb” for consistency with previous
55 literature.

56 Metatranscriptomics is one strategy for gleaning information about microbial activity in
57 the environment. *Ca. Poseidoniales* transcripts can be abundant in marine metatranscriptomes,
58 suggesting transiently high transcriptional activity [17,18]. When metatranscriptome reads from
59 the Gulf of Aqaba were mapped to metagenomic contigs from the Mediterranean Sea, genes
60 involved in amino acid transport, carbon metabolism, and cofactor synthesis were highly
61 transcribed in the aggregate euryarchaeal community [19,20]. In another study, mapping deep-

62 sea metatranscriptome reads to novel *Ca. Poseidoniales* MAGs indicated transcription of genes
63 related to protein, fatty acid, and carbohydrate transport and metabolism, likely fueling aerobic
64 heterotrophy [21]. Finally, a metaproteomics study found that euryarchaeal transport proteins for
65 L-amino acids, branched-chain amino acids, and peptides were present throughout the Atlantic
66 Ocean [22]. Despite these advances, little is known about similarities or differences in gene
67 transcription between *Ca. Poseidoniales* and *Thalassarchaeaceae*.

68 We report MAG-resolved metatranscriptomic analyses of *Ca. Poseidoniales* in coastal
69 waters near Sapelo Island (GA, USA). Prior work suggested *Ca. Poseidoniales* are sporadically
70 active at Sapelo Island [23] and may comprise the majority of archaea in mid-shelf surface
71 waters of the South Atlantic Bight (SAB) [24]. Since other studies thoroughly described the
72 genomic content of *Ca. Poseidoniales* MAGs, our focus instead was determining which clades
73 were transcriptionally active and identifying highly or differentially transcribed genes. We used
74 two Sapelo Island MAGs [25] combined with recent marine MAG collections [15,16] to
75 competitively recruit reads from a metatranscriptomic time series [26] and an incubation
76 experiment [23] to determine which clades were active over time. We then used representative
77 MAGs from highly active genera to determine which *Ca. Poseidoniales* genes were transcribed.
78 Finally, we used quantitative PCR (qPCR) to measure the abundance of *Ca. Poseidoniales* 16S
79 rRNA genes in DNA samples throughout the SAB to assess the prevalence *Ca. Poseidoniales* in
80 this region.

81

82 **MATERIALS AND METHODS**

83 **PHYLOGENOMICS**

84 Phylogenomic analyses compared SIMO Bins 19-2 and 31-1 (ref. 25) to previously-
85 reported *Ca. Poseidoniales* MAGs [15,16]. Average nucleotide identity (ANI) was calculated
86 using fastANI [27] to compare the set of non-redundant MAGs from Tully [16] to 15 Port
87 Hacking MAGs [15] and the two SIMO MAGs; MAGs with ANI <98.5% were added to the
88 non-redundant set. Phylogenomic analysis was conducted using a set of sixteen ribosomal
89 proteins [28] within anvi'o v4 (ref. 29). All genomes were converted to contig databases and
90 ribosomal proteins were identified using HMMER [30]. These proteins were concatenated,
91 aligned using MUSCLE [31], and used to build a phylogenomic tree using FastTree [32] within
92 anvi'o.

93

94 COMPETITIVE READ MAPPING

95 We used competitive read mapping [33] to determine which *Ca. Poseidoniales* genera
96 were transcriptionally active in free-living Sapelo Island metatranscriptomes [23,26]. Analyses
97 of “field” communities included Gifford et al. metatranscriptomes (iMicrobe Accession
98 [CAM_P_0000917](https://www.ncbi.nlm.nih.gov/trace/assembly/0000917)) [26] and the T₀ metatranscriptomes from Vorobev et al. [23], while dark
99 incubation analyses included only Vorobev et al. samples (T₀ and T₂₄; NCBI BioProject
100 [PRJNA419903](https://www.ncbi.nlm.nih.gov/trace/assembly/0000917)). Temperature, salinity, dissolved oxygen, pH, and turbidity data corresponding
101 to metatranscriptome sampling times were downloaded from the NOAA National Estuarine
102 Research Reserve System website (<http://cdmo.baruch.sc.edu>; last accessed 16 July 2020).

103 Contigs from all MAGs from the phylogenomic analysis were used as a database for read
104 mapping using Bowtie2 v.2.2.9 (ref. 34) with the “very-sensitive” flag. Samtools v.1.3.1 (ref. 35)
105 was used to index resulting BAM files, which were then profiled and summarized in anvi'o.
106 Contig genus identity was imported to the anvi'o contig database as an external collection. The

107 number of transcripts L^{-1} was calculated by scaling the number of mapped reads by the volume
108 of water filtered and the recovery of internal standards (reported in [23,26]) as previously
109 described [36]. Seasonal transcript abundances were compared using a one-way ANOVA test in
110 R [37] with data log-transformed as necessary to improve normality. When ANOVA results were
111 significant, groupings were defined post-hoc with Tukey's Honest Significant Difference (HSD)
112 test using the agricolae R package [38].

113 Non-metric multidimensional scaling (NMDS) analysis of metatranscriptome hits was
114 conducted using the vegan R package [39]. NMDS input was a distance matrix constructed by
115 Hellinger-transforming the table of transcript hits and calculating Euclidean distance between
116 samples [40]. Genus vectors were calculated using the *envfit* command. Significance of
117 groupings were tested by permutational multivariate analysis of variance (the *adonis* command)
118 with 999 permutations.

119

120 MAG-SPECIFIC ANNOTATION AND TRANSCRIPT ANALYSIS

121 Gene-specific analyses focused on three MAGs: two from the SIMO collection (SIMO
122 Bin 19-2, Genbank: [VMDE00000000](#); SIMO Bin 31-1, [VMBU00000000](#); [25]) and one (RS440,
123 [PBUZ00000000](#); [41]) binned from TARA Oceans metagenomes [42]. These MAGs represented
124 genera O1, O3, and M, respectively, which were highly abundant in metatranscriptomes (see Fig.
125 1). RS440 was selected due to a high number of transcripts recruited when genus M was
126 abundant (data not shown).

127 MAGs were annotated using the archaeal database in Prokka v.1.13 (ref. 43), using
128 DIAMOND [44] to search against all orthologous groups in eggNOG-mapper v.1 (refs. 45, 46),
129 and using the online BlastKOALA portal (<https://www.kegg.jp/blastkoala/>, last accessed 6

130 March 2019) [47]. Putative genes for carbohydrate-active enzymes, peptidases, and membrane
131 transport proteins were identified using HMMER searches of dbCAN2 (HMMdb v.7) [48,49],
132 *MEROPS* v.12.0 (ref. 50), and the Transporter Classification Database [51], respectively.

133 Transcript reads were mapped to MAGs (combined into a single database such that each
134 read mapped to only one MAG) to identify *Ca. Poseidoniales* genes that were highly or
135 differentially transcribed. Coverage was calculated by profiling BAM files in `anvi'o` and
136 normalized to coverage per million reads (CPM) by dividing by the total number of reads per
137 sample. For each MAG, “highly transcribed” genes were the 5% of putative genes with the
138 highest median CPM across metatranscriptomes (SIMO Bin 19-2: 63 genes, SIMO Bin 31-1: 70
139 genes, RS440: 77 genes).

140 DESeq2 v.3.11 (ref 52) was used to identify genes from each MAG that were
141 differentially transcribed when each genus was highly transcriptionally active. For each MAG,
142 “treatment” samples in DESeq2 were those where the respective genus recruited $\geq 50\%$ of *Ca.*
143 *Poseidoniales* reads from the metatranscriptome. Thus, positive fold-change values are genes
144 transcribed at higher levels when the genus is highly transcriptionally active (compared to other
145 metatranscriptomes). DESeq2 was also used to identify differentially transcribed genes for each
146 MAG between T_0 and T_{24} samples in high tide (HT) dark incubations [23]. Since T_{24} samples
147 were the “treatment” condition in DESeq2, positive fold-change values here are genes
148 transcribed at higher levels in T_{24} compared to T_0 samples. In all DESeq2 analyses, genes with
149 Benjamini-Hochberg adjusted $p < 0.1$ were counted as having significantly different transcription.

150

151 16S rRNA QUANTITATIVE PCR

152 DNA samples from SAB field campaigns in 2014 and 2017 [24,53] were used as
153 templates for qPCR reactions targeting the *Ca. Poseidoniales* 16S rRNA gene. Samples included
154 the variety of shelf habitats (inshore, nearshore, mid-shelf, shelf-break, and oceanic as previously
155 defined [24]; Fig. S1). Primers were GII-554-f [54] and Eury806-r [55] with cycling conditions
156 as previously reported [56] (Table S1). Reactions (25 μ L, triplicate) used iTaq Universal Green
157 SYBR Mix (Bio-Rad, Hercules, CA) in a C1000 Touch Thermal Cycler/CFX96 Real-Time
158 System (Bio-Rad, Hercules, CA). Each plate included a no-template control and a standard curve
159 (serial dilutions of a linearized plasmid containing a previously-sequenced, cloned amplicon).
160 Abundance of *Ca. Poseidoniales* 16S rRNA genes was compared to published bacterial 16S
161 rRNA gene abundance from the same samples [24,53]. Regional variability of gene abundance
162 was assessed using a one-way ANOVA and a post-hoc HSD test as described above. Model II
163 regressions of log-transformed qPCR data were estimated using the lmodel2 R package [57] as
164 previously described [53]. All plots were constructed with *anvi'o* or the ggplot2 R package [58].

165

166 **RESULTS**

167 EURYARCHAEOTAL MAGs

168 SIMO Bins 19-2 and 31-1 were estimated as 82.5-92.3% and 77.5-96.2% complete,
169 respectively, with redundancy <0.6% [25]. Phylogenomics placed both in the putative family *Ca.*
170 *Thalassarchaeaceae* (MGIIb) and genera O1 (SIMO Bin 19-2) and O3 (SIMO Bin 31-1; Fig. S2).
171 Phylogenomic groupings were generally consistent with previous findings [15,16].

172 Both SIMO MAGs contained a proteorhodopsin gene. Presence of a methionine residue
173 at position 315 suggested absorption of green light [59,60], and both proteorhodopsin genes
174 grouped in “Archaea Clade B” [11,16,61] (Fig. S3). Both MAGs included partial or complete

175 pathways indicating aerobic heterotrophic growth, such as glycolysis, the TCA cycle, and
176 electron transport chain components (Table S2). Pathways for metabolism of compounds such as
177 fatty acids, peptides, and proteins were also present, as were transport systems and metabolic
178 pathways for amino acids and nucleotides.

179

180 DOMINANT GENERA IN FIELD METATRANSCRIPTOMES

181 There were significant seasonal differences in transcript recruitment by the combined set
182 of *Ca. Poseidoniales* MAGs ($F_{3,28}=4.9$, $p=0.007$): most summer samples had $>10^{10}$ *Ca.*
183 *Poseidoniales* transcripts L^{-1} , significantly more than in other seasons (Fig. 1A,C; Table S3). The
184 diversity of transcriptionally-active *Ca. Poseidoniales* also changed seasonally. Genera O1 and
185 O3 accounted for most reads mapped from summer samples (typically 89.5-99.5% of *Ca.*
186 *Poseidoniales* reads), with most mapping to O1 (Fig. 1A,B). HT (and not low tide; LT)
187 metatranscriptomes from July 2014 also had a moderate fraction of reads (37.5-39.6%) mapped
188 to *Ca. Poseidoniaceae*. In contrast to summer samples, November 2008 and May 2009 transcripts
189 were predominantly O3, while those from February 2009 and October 2014 were mostly *Ca.*
190 *Poseidoniaceae* genera M, L1, or L2 (Fig. 1A, Table S3). NMDS analysis showed clear seasonal
191 groupings (PERMANOVA: $r^2=0.693$, $p=0.001$; Fig. S4).

Euryarchaeal transcriptomes in the coastal ocean

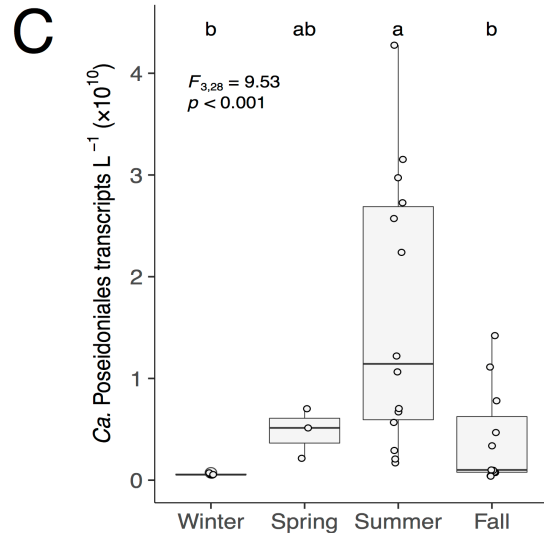
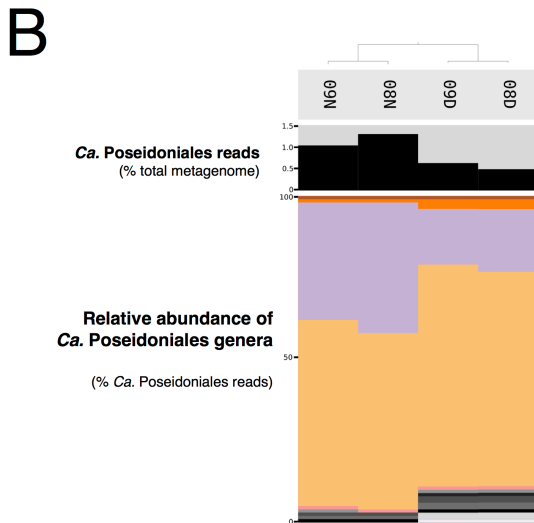
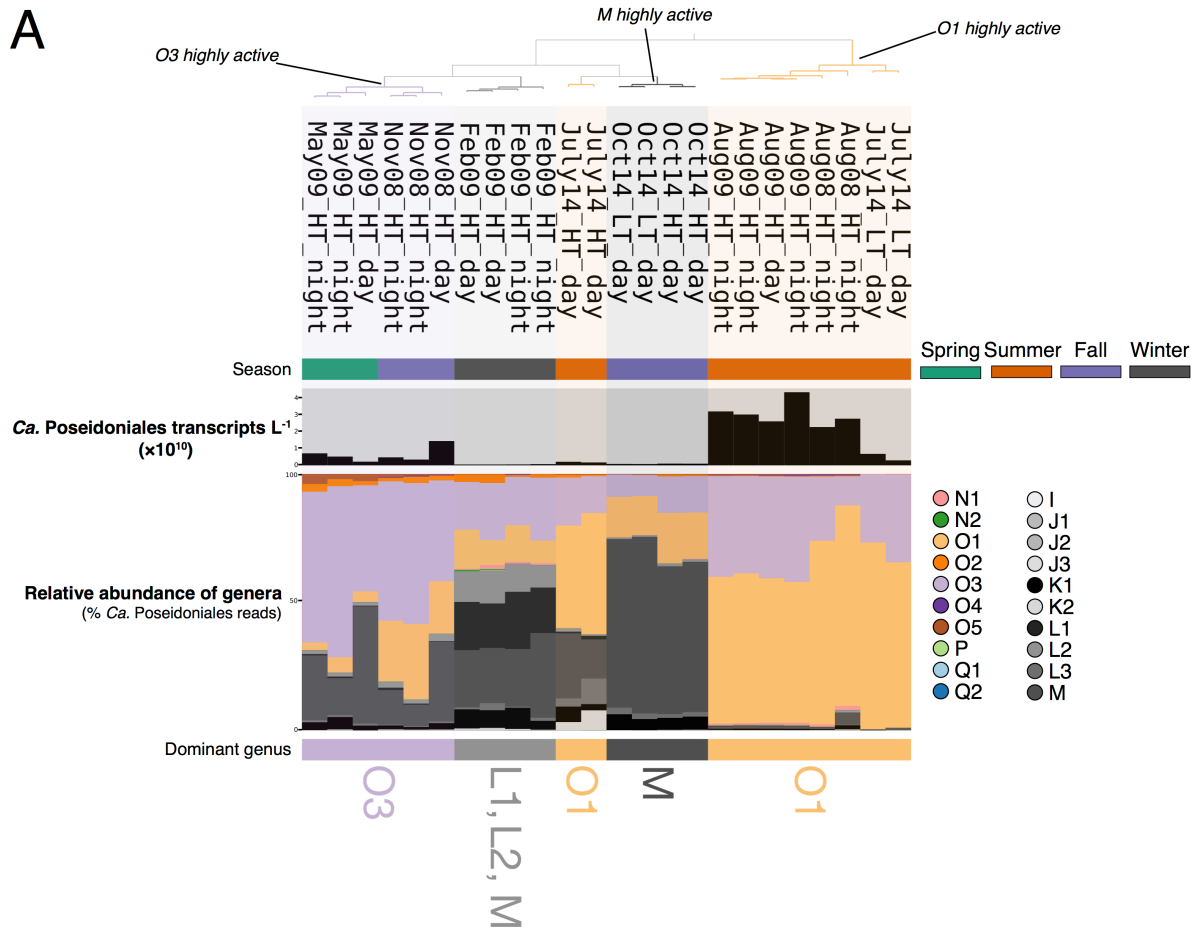


Fig. 1A) Relative abundance of *Ca. Poseidoniales* genera in Sapelo Island metatranscriptomes ($n=24$). The dendrogram (top) shows grouping by similarity. Season is indicated by color beneath sample names. The bar chart shows the abundance of *Ca. Poseidoniales* transcripts L^{-1} and the stacked bar charts show the relative abundance of genera (% total *Ca. Poseidoniales* transcripts), colored by genus. Dominant genera are indicated below the stacked bar chart. “Highly active” samples for each genus are marked and were used for analysis of differential transcription. **B)** Relative abundance of genera in Sapelo Island metagenomes ($n=4$), as described above. Since internal standards were not included in metagenomes, total *Ca. Poseidoniales* reads are shown as a percentage of the total metagenome. **C)** Boxplots of *Ca. Poseidoniales* reads L^{-1} , grouped by season (winter, $n=4$; spring, $n=3$; summer, $n=10$; fall, $n=7$). Values from individual metatranscriptomes are overlain. Results of an ANOVA are indicated; letters at the top indicate post-hoc groups according to Tukey’s HSD test.

192

193

194 HIGHLY TRANSCRIBED *Ca.* POSEIDONIALES GENES

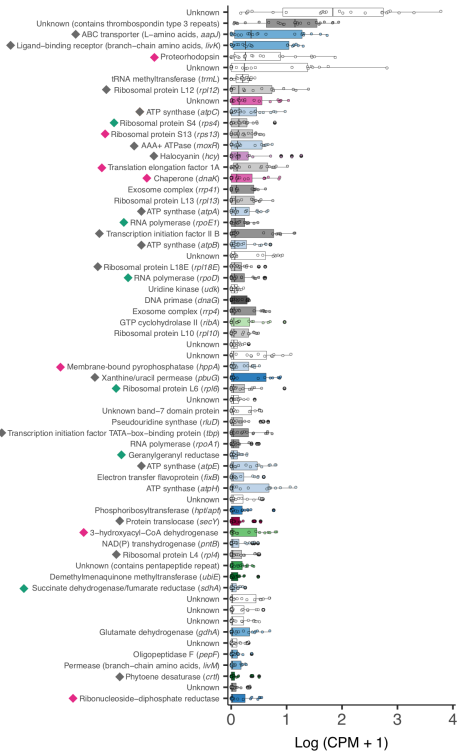
195 Many highly transcribed *Ca.* Thalassarchaeaceae (MGIIb) genes were involved in
196 translation, transcription, replication/repair, or post-translation protein modification (Fig. 2).
197 Genes encoding proteins involved in energy production or conservation (ATPases, a
198 pyrophosphate-energized proton pump, and proteorhodopsin) were also highly transcribed.
199 Notably, the *aapJ* and *livK* genes, encoding substrate-binding proteins of L-amino acid and
200 branch-chain amino acid transporters, respectively, were among the most highly transcribed
201 genes in both *Ca.* Thalassarchaeaceae MAGs (Fig. 2, Table S2).

202 Many of the highly transcribed genes mapping to the *Ca.* Poseidoniaceae (MGIIa) MAG
203 were not highly transcribed by *Ca.* Thalassarchaeaceae, including genes encoding a carbamoyl
204 phosphate synthetase subunit (*carA*), a family 2 glycosyl transferase, chromosomal protein
205 MC1b, and a *ftsX*-like permease. The *carA* gene had the highest median coverage of *Ca.*
206 Poseidoniaceae genes across coastal metatranscriptomes (Fig. 2, Table S2). While both *Ca.*
207 Thalassarchaeaceae MAGs also contained the carbamoyl phosphate synthetase genes, neither
208 transcribed *carA* at high levels (Table S2).

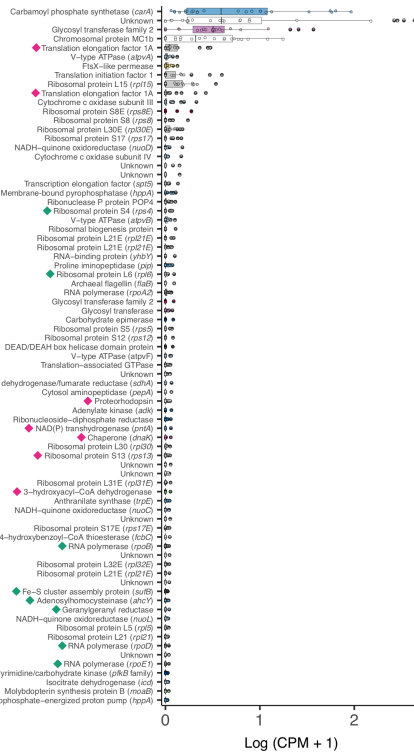
209 Twelve genes were highly transcribed by *Ca.* Thalassarchaeaceae and not by *Ca.*
210 Poseidoniaceae, including genes encoding ATP synthase, transcription initiation factor IIB,
211 halocyanin, phytoene desaturase, protein translocase, xanthine/uracil permease, and receptors for
212 amino acid transporters (Fig. 2, Table S2). Other than those encoding ribosomal proteins, only
213 six genes were highly transcribed in all three MAGs: a chaperone protein, a ribonucleoside-
214 diphosphate reductase, translation elongation factor 1A, 3-hydroxyacyl-CoA dehydrogenase, a
215 membrane-bound pyrophosphatase (*hppA*), and proteorhodopsin (Fig. 2).

SIMO Bin 19-2 (O1; *Ca. Thalassarchaeaceae*)

SIMO Bin 31-1 (O3; *Ca. Thalassarchaeaceae*)



RS440 (M; *Ca. Poseidoniaceae*)



Highly transcribed in:

- ◆ All 3 MAGs
- ◆ *Ca. Thalassarchaeaceae* (MGIb) MAGs only
- ◆ One *Ca. Thalassarchaeaceae* (MGIb) and one *Ca. Poseidoniaceae* (MGIa) MAG

COG

- D: cell cycle control
- M: cell wall/membrane biogenesis
- O: post-translational/protein modification/chaperones
- T: signal transduction
- U: intracellular trafficking/secretion
- J: translation
- K: transcription
- L: cell replication/repair
- C: energy production/conservation
- E: amino acid metabolism/transport
- F: nucleotide metabolism/transport
- G: carbohydrate metabolism/transport
- H: coenzyme metabolism
- I: lipid metabolism
- P: inorganic ion transport/metabolism
- Q: secondary structure
- S: unknown function
- None assigned

Fig. 2 Boxplots of highly-transcribed MAG genes (top 5%) in Sapelo Island field metatranscriptomes. Overlain points show CPM for individual metatranscriptomes ($n=24$). Shading indicates COG functional category assigned by eggNOG-mapper (genes assigned to group S were similar to proteins of unknown function in the COG database, while genes with no COG assignment did not match proteins in the COG database). Diamonds indicate genes highly transcribed in all MAGs (pink), in *Ca. Thalassarchaeaceae* (MGIb) MAGs only (gray), or in the *Ca. Poseidoniaceae* (MGIa) MAG and one *Ca. Thalassarchaeaceae* MAG (green).

218 DIFFERENTIAL GENE TRANSCRIPTION

219 We were interested in identifying genes with variable transcription levels when genera
 220 O1, O3, and M were highly transcriptionally active in the ocean. Twenty-three genes were
 221 differentially transcribed in O1-active samples (Fig. 3, Table S4), sixteen of which had higher
 222 abundance in O1-active metatranscriptomes compared to other metatranscriptomes. These highly
 223 transcribed genes encoded proteorhodopsin, two copper-containing redox proteins (halocyanin
 224 and plastocyanin), and proteins involved in lipid metabolism (3-hydroxyacyl-CoA

225 dehydrogenase and oligosaccharyltransferase), nucleotide transport/metabolism (ribonucleotide-
 226 diphosphate reductase and xanthine/uracil permease), and amino acid transport (ligand-binding
 227 receptor for a L-amino acid transporter,

228 *aapJ*). Differentially transcribed genes
 229 mapping to the O3 MAG were mostly
 230 depleted in O3-active
 231 metatranscriptomes and largely encoded

232 proteins of unknown function; only the
 233 gene encoding ribosomal protein L12

234 was enriched in O3-active samples (Fig.
 235 S5, Table S4). Only four genes

236 mapping to the M MAG were

237 differentially transcribed in M-active metatranscriptomes. Annotated genes encoded

238 chromosomal protein MC1b, an ATPase subunit, and a glycosyl transferase, which all had

239 significantly fewer transcripts in M-rich samples (Fig. S6, Table S4). One gene of unknown

240 function was enriched compared to other samples.

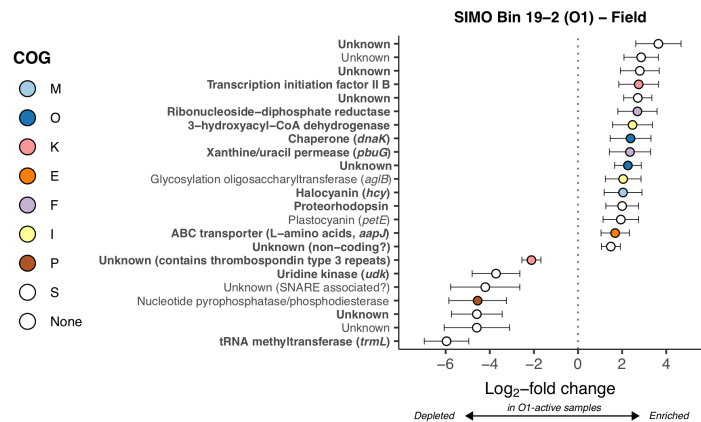


Fig. 3 Log₂-fold change of SIMO Bin 19-2 (genus O1) genes differentially transcribed in field metatranscriptomes where transcriptional activity of *Ca. Poseidoniales* was dominated by genus O1 (see Fig. 1, Table S3), calculated with DESeq2. Error bars show estimated standard error. Only genes with adjusted *p*-values < 0.1 are shown. Color indicates COG functional category (see Fig. 2). Bold indicates genes in the top 5% median transcript coverage across field metatranscriptomes (Fig. 2).

241

242 DARK INCUBATION METATRANSCRIPTOMES

243 Incubation had little effect on transcription by the dominant genera in LT samples (Fig. 4,
244 Table S3). In contrast, there were distinct shifts in transcriptionally active populations during
245 incubations of all HT samples. July HT metatranscriptomes initially contained 60.4-62.5% *Ca.*
246 *Thalassarchaeaceae* (MGIIb) while hits from the corresponding T₂₄ samples were 98.1-99.3%
247 *Ca. Thalassarchaeaceae*, due to increased transcript hits to genus O1 (Fig. 4, Table S3).
248 Likewise, October 2014 HT samples initially contained 65.0-66.6% hits to *Ca. Poseidoniacae*
249 (MGIIa) but changed to 78.3-98.8% hits to *Ca. Thalassarchaeaceae* at T₂₄ due to an increase in
250 hits to O1 (Fig. 4).

251 DESeq2 identified 40 differentially
252 transcribed genes mapping to the O1 MAG
253 between HT T₀ and T₂₄ metatranscriptomes.

254 Four O1 genes had higher transcription at
255 T₂₄, including xanthine/uracil permease
256 (*pbuG*) and an amino acid transporter

257 substrate-binding domain (*aapJ*; Fig. 5,
258 Table S5). The 36 O1 genes transcribed
259 at lower levels encoded proteins

260 involved in repair of UV-damaged

261 DNA, amino acid or nucleotide metabolism, coenzyme synthesis, peptidases or proteases,

262 transcription, DNA replication, and lipid biosynthesis, as well as phytoene desaturase (*crtD*) and

263 multiple subunits of pyruvate dehydrogenase (*pdhC*, *pdhA*). None of the genes mapping to the

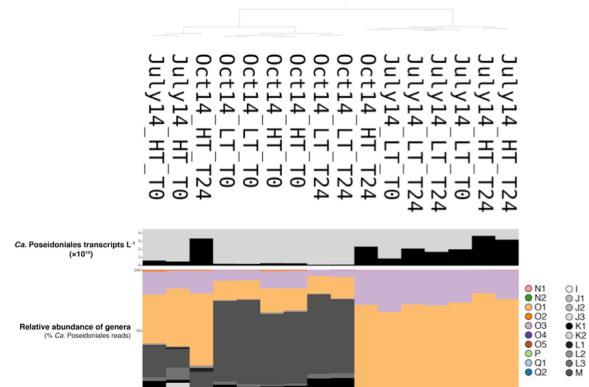


Fig. 4 Comparisons of competitive read mapping to *Ca. Poseidoniales* genera at the beginning and end of 24-hour incubations of Sapelo Island water conducted by [23]. The dendrogram (top) shows grouping by similarity. The bar chart below the dendrogram is the abundance of *Ca. Poseidoniales* transcripts L⁻¹. Stacked bar charts show the relative abundance of genera (% total *Ca. Poseidoniales* transcript reads), colored by genus.

264 O3 or M MAGs were transcribed at significantly different levels between HT incubation
 265 timepoints ($p>0.1$ for all genes; Table S5).

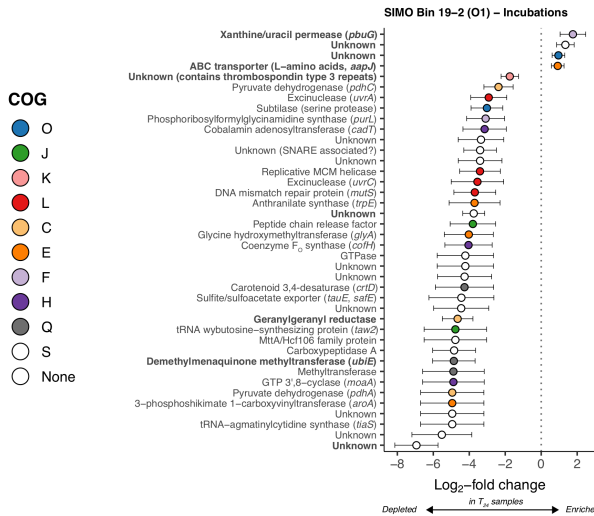


Fig. 5 Log₂-fold change of SIMO Bin 19-2 (genus O1) genes differentially abundant in T₂₄ versus T₀ metatranscriptomes from Sapelo Island high tide waters. Error bars show estimated standard error. Only genes with adjusted p -values < 0.1 are shown. Color indicates COG functional category (see Fig. 2). Bold indicates genes in the top 5% median transcript coverage across field metatranscriptomes (Fig. 2).

266
 267 16S rRNA GENE ABUNDANCE

268 *Ca. Poseidoniales* 16S rRNA genes were detected in all SAB DNA samples ($n=208$),
 269 with a range from 1.6×10^4 to 7.6×10^8 genes L⁻¹ (Table S6). Standard curves for the *Ca.*
 270 *Poseidoniales* assay always had $r^2 > 0.99$ (mean \pm standard deviation: 0.99 ± 0.001) and the mean
 271 efficiency was 93.4% ($\pm 2.0\%$; Table S1). When data from all cruises were combined, *Ca.*
 272 *Poseidoniales* genes were most abundant throughout inshore and nearshore waters and least
 273 abundant in shelf-break and oceanic samples ($F_{4,204} = 18.5$, $p < 0.001$; Fig. 6A). There was a strong
 274 linear relationship between log-transformed bacterial and *Ca. Poseidoniales* 16S rRNA gene
 275 abundances, with bacterial abundances 2-3 orders of magnitude higher (Fig. 6B).

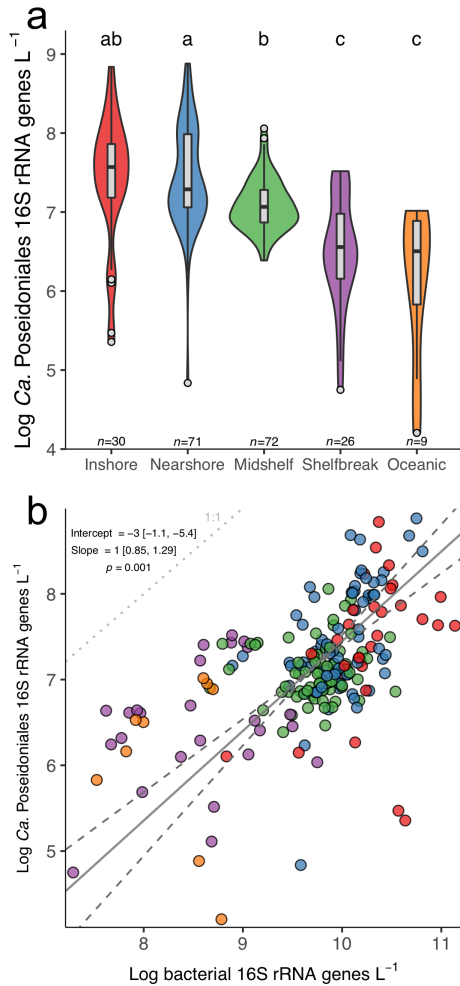


Fig. 6 A) Violin plots of log-transformed *Ca. Poseidoniales* 16S rRNA gene abundances across regions in the SAB, with overlain boxplots. Width of the violin plot corresponds to data probability density. Color denotes sampling region. Letters above boxes denote post-hoc grouping according to Tukey's HSD test. B) Scatterplot of bacterial and *Ca. Poseidoniales* 16S rRNA gene abundances in the SAB. The solid line shows the best fit of a model II (major axis) linear regression, with dashed lines showing a 95% confidence interval of the slope. Regression parameters are shown on the plot.

276

277 DISCUSSION

278 ABUNDANCE OF *CA. POSEIDONIALES* GENES IN THE SOUTH ATLANTIC BIGHT

279 The abundance of *Ca. Poseidoniales* 16S rRNA genes in the coastal SAB is among the

280 highest measured in the ocean, with nearly 10⁹ genes L⁻¹ in some samples. Typical *Ca.*

281 *Poseidoniales* abundance is 10⁶-10⁷ genes or cells L⁻¹ in oligotrophic waters [62-66] and 10⁷-10⁸

282 genes or cells L⁻¹ in coastal waters [9,54,56,67-69]. Greater gene abundance in inshore,

283 nearshore, and mid-shelf waters indicates *Ca. Poseidoniales* are more abundant over the shallow

284 shelf than further offshore (Fig. 6A), matching clone library data from the SAB [24] and data

285 from the Central California Current and the Black Sea [9,68]. The DOM in productive, turbid

286 SAB coastal waters supports highly active heterotrophic microbial populations [70,71]. Our data
287 suggest large populations of *Ca. Poseidoniales* are part of this heterotrophic community, and the
288 correlation between *Ca. Poseidoniales* and bacterial abundance (Fig. 6B) suggests common
289 factors influence the abundance of these populations.

290

291 TRANSCRIPTIONALLY ACTIVE *CA. POSEIDONIALES*

292 While numerous studies have demonstrated high abundance of *Ca. Poseidoniales* in the
293 coastal ocean (e.g., [56,69]), little is known about which clades are transcriptionally active in
294 these regions. At Sapelo Island, the striking dominance of the *Ca. Thalassarchaeaceae* (MGIIb)
295 genera O1 and O3 in summer samples, which also contained the highest amount of aggregate *Ca.*
296 *Poseidoniales* transcripts (Fig. 1), indicates that *Ca. Thalassarchaeaceae* are highly-active during
297 the summertime. Outliers to this pattern were July 2014 HT samples, which contained abundant
298 *Ca. Poseidoniaceae* (MGIIa) transcripts (though *Ca. Thalassarchaeaceae* still comprised the
299 majority of their *Ca. Poseidoniales* reads). A previous study found relatively high salinity and
300 DOM enriched in marine-origin molecules over the mid-shelf SAB during July 2014 [72]. Our
301 data suggest *Ca. Poseidoniaceae* were relatively active over the shelf during this time and were
302 transported inshore during flood tides, leading to shifts in transcriptional diversity between LT
303 waters (dominated by *Ca. Thalassarchaeaceae*) and HT waters (which included a higher number
304 of *Ca. Poseidoniaceae*).

305 *Ca. Poseidoniaceae* (MGIIa) are the predominant euryarchaeal family in many coastal
306 ecosystems, particularly in summer (e.g., [9,14,56,73,74]), but it is unclear what general patterns
307 govern *Ca. Poseidoniales* distributions in coastal waters worldwide. Studies of *Ca. Poseidoniales*
308 ecology often focus on distributions with depth, typically finding abundant *Ca.*

309 Thalassarchaeaceae (MGIIb) in deeper waters and *Ca. Poseidoniaceae* (MGIIa) more prevalent
310 in euphotic waters (e.g., [12,54,75-77]). A recent mapping of global ocean metagenome reads
311 showed that coastal populations of *Ca. Poseidoniales* were primarily *Ca. Poseidoniaceae*, though
312 *Ca. Thalassarchaeaceae* MAGs recruited a substantial number of reads from some coastal
313 metagenomes [16]. Our data match this latter pattern, with *Ca. Poseidoniales* populations in
314 surface waters off Sapelo Island dominated by highly active *Ca. Thalassarchaeaceae* (Fig. 1).
315 The higher abundance of MAGs from genera O1 and O3 (also referred to as MGIIb.12 and
316 MGIIb.14) in some mesopelagic and coastal samples with relatively high temperature (~23–
317 30°C; [16]) may explain the unusual pattern found in SAB waters: these genera peaked in
318 summer at Sapelo Island, when water temperatures were 29–30°C (Table S2), suggesting they
319 may be adapted to growth at relatively low light and high temperature.

320

321 *CA. POSEIDONIALES* GENE TRANSCRIPTION PATTERNS

322 Sapelo Island metatranscriptome reads that mapped to *Ca. Poseidoniales* were analyzed
323 in three ways:

- 324 (1) We determined sets of “highly transcribed” genes mapping to MAGs of
325 transcriptionally-active *Ca. Poseidoniales* genera (5% of MAG genes with the highest
326 median transcript coverage);
- 327 (2) We identified genes mapping to *Ca. Poseidoniales* MAGs that were differentially
328 transcribed when its genus was highly active ($\geq 50\%$ of *Ca. Poseidoniales* transcripts
329 in a sample; Fig. 1, Table S2);
- 330 (3) We identified genes mapping to *Ca. Poseidoniales* MAGs that were differentially
331 transcribed at the beginning versus end of dark incubations. Since dark incubation

332 separates indigenous microbes from light and sources of short-lived substrates,
333 transcription of corresponding transporters and metabolic genes ceases during
334 incubations as substrates are consumed. We therefore assume transcript depletion in
335 T₂₄ compared to T₀ metatranscriptomes indicates genes that were transcriptionally
336 active in the field [23]. This interpretation was bolstered by significant transcript
337 depletions for genes involved in repairing UV damage to DNA (*uvrA*, *uvrC*, and
338 *cofH*; Fig. 5), an expected result given alleviation of UV stress in dark incubations.

339
340 In the following sections, we synthesize these analyses to discuss *Ca. Poseidoniales*
341 transcriptional activity related to metabolism of labile DOM, transport/metabolism of amino
342 acids and nucleotides, and basic energetic processes. Though lack of a cultivated representative
343 limits the analysis to computationally-inferred functions, these data provide hypotheses
344 regarding the activity of *Ca. Poseidoniales* families in the coastal ocean.

345

346 PROTON GRADIENTS AND ELECTRON TRANSPORT

347 Our analysis revealed that *Ca. Poseidoniales* genes involved in establishing
348 transmembrane proton gradients were highly transcribed in our samples. Genes encoding
349 proteorhodopsin were among the most highly transcribed by both *Ca. Thalassarchaeaceae* MAGs
350 and were highly transcribed in O1-active samples (Figs. 2,3). Proteorhodopsins consist of a
351 retinal chromophore linked to a transmembrane protein and use light energy to pump protons
352 across the cell membrane [78]. The resulting energy can be coupled to ATP production or other
353 chemiosmotic processes and often supports photoheterotrophy, though its function varies widely
354 [61]. Proteorhodopsin genes are highly transcribed in the photic zone of both open ocean and

355 coastal waters (e.g., [79-81]) and our data indicate coastal *Ca.* Poseidoniales conform to this
 356 pattern, consistent with recent evidence from other regions [20,82,83]. High transcription of
 357 proteorhodopsin supports the photoheterotrophic lifestyle hypothesized for *Ca.* Poseidoniales
 358 (e.g., [9,11,12,15,16]).

359 Since O1 proteorhodopsin transcript abundance did not differ between the beginning and
 360 end of dark incubations (Fig. 5), light may not regulate *Ca.* Thalassarchaeaceae proteorhodopsin
 361 transcription. However, depletion of O1 *crtD* (carotenoid 3,4-desaturase) transcripts during dark
 362 incubation (Fig. 5) suggests light may regulate retinal synthesis. Whether proteorhodopsin
 363 transcription responds to light varies among marine bacteria [60,84,85], and the function of
 364 constitutive transcription is not straightforward: while some bacteria use proteorhodopsin to
 365 produce ATP when carbon-limited [86], high amounts of proteorhodopsin in other bacteria can
 366 physically stabilize membranes even when inactive [87]. The high proteorhodopsin transcription
 367 in our data emphasizes, but provides little mechanistic clarification of, the physiological role for
 368 proteorhodopsin in *Ca.* Poseidoniales (Table 1).

Table 1 Transcriptional traits shared or distinct among euryarchaeal families¹

Putative function	Relevant gene(s)	Distribution	Evidence
Proteorhodopsin	Proteorhodopsin gene	Both families	Highly transcribed (Fig. 2); enriched when O1 active (Fig. 3)
Pyrophosphatase	<i>hppA</i>	Both families	Highly transcribed (Fig. 2)
Protease/peptidase	<i>pepF</i> , <i>lonB</i> , <i>pepA</i> , <i>pip</i> , carboxypeptidase A, subtilase	Both families	Highly transcribed (Fig. 2); depletion during dark incubation (Fig. 5)
β-oxidation	3-hydroxyacyl-CoA dehydrogenase	Both families	Highly transcribed (Fig. 2); enriched when O1 active (Fig. 3)
Proteorhodopsin retinal synthesis	<i>crtI</i> , <i>crtD</i>	<i>Ca.</i> Thalassarchaeaceae only	Highly transcribed in SIMO MAGs (Fig. 2); depletion during dark incubation (Fig. 5)
Electron transport	Halocyanin gene	<i>Ca.</i> Thalassarchaeaceae only	Highly transcribed in SIMO MAGs (Fig. 2); enriched when O1 active (Fig. 3)
Amino acid transport/metabolism	<i>aapJ</i> , <i>livK</i> , <i>aroA</i> , <i>trpE</i>	<i>Ca.</i> Thalassarchaeaceae only	Highly transcribed (Fig. 2); depletion during dark incubation (Fig. 5)
Xanthine/uracil permease	<i>pbuG</i>	<i>Ca.</i> Thalassarchaeaceae only	Highly transcribed (Fig. 2); enriched when O1 active (Fig. 3); depletion during incubations (Fig. 5)
Amino acid synthesis	<i>carA</i>	<i>Ca.</i> Poseidoniaceae only	Highly transcribed (Fig. 2)
Carbohydrate synthesis	Family 2 glycosyl transferase	<i>Ca.</i> Poseidoniaceae only	Highly transcribed (Fig. 2)

¹Putative *Ca.* Poseidoniales families are *Ca.* Poseidoniaceae (MGIIb; MAG RS440) and *Ca.* Thalassarchaeaceae (MGIIb; SIMO Bins 19-2, 31-1).

369
 370 Numerous genes encoding putative electron transport proteins were highly transcribed by
 371 at least one *Ca.* Poseidoniales family (Fig. 2). Like proteorhodopsin, a halocyanin gene was

372 among the most highly transcribed *Ca. Thalassarchaeaceae* genes and was enriched when genus
373 O1 was transcriptionally active (Fig. 3). Halocyanins are involved in the electron transport chain
374 and have been posited to increase the energy yield of aerobic respiration in *Ca.*
375 *Thalassarchaeaceae* to stimulate rapid growth [12]. The similar transcription patterns of
376 proteorhodopsin and halocyanin suggests proteorhodopsin activity in coastal *Ca.*
377 *Thalassarchaeaceae* may function to increase growth rates during respiration, aiding rapid
378 population growth when conditions permit.

379 The *hppa* gene from all *Ca. Poseidoniales* MAGs was highly transcribed (Fig. 2; Table 1).
380 The gene putatively encodes a membrane-bound pyrophosphatase, which generates a proton
381 gradient via hydrolysis of pyrophosphate, a byproduct of numerous cellular processes [88]. In
382 metatranscriptomes from a phytoplankton bloom, enrichment of *hppA* transcripts suggested high
383 pyrophosphate-based energy conservation in oligotrophic waters [89]. Similarly, *hppA* was
384 abundant in metatranscriptomes from Lake Llebre, particularly at night [90]. Although *hppA* is
385 widespread in MAGs from *Ca. Poseidoniales* [15] it has not been recognized as a potentially
386 important part of their metabolism. Our data suggest *Ca. Poseidoniales* may be capable of using
387 pyrophosphatase (along with proteorhodopsin) to generate a protonmotive force (Table 1).

388

389 POTENTIAL IMPORTANCE OF MARINE DOM IN *CA. POSEIDONIALES* METABOLISM

390 Although the T₀ metatranscriptomes from summer versus fall were dominated by
391 transcripts from different *Ca. Poseidoniales* families, a 24-hour dark incubation consistently
392 favored transcription by *Ca. Thalassarchaeaceae* when samples were collected at HT (Fig. 4).
393 This tidal stage-linked increase in *Ca. Thalassarchaeaceae* transcription could relate to
394 differences in DOM availability between HT and LT, consistent with numerous studies

395 implicating DOM in shaping *Ca. Poseidoniales* populations [9,10,91]. The HT Sapelo Island
396 DOM pool is primarily of marine origin while LT DOM is more riverine- and marsh-derived
397 [72], which may select for growth of different *Ca. Poseidoniales* families in the water masses
398 present at different tidal stages. Furthermore, the depletion of transcripts encoding two pyruvate
399 dehydrogenase subunits (*pdhA* and *pdhC*) during incubations (Fig. 5) suggests *Ca. Poseidoniales*
400 were metabolizing phytoplankton photosynthate *in situ*. Alternatively, these tidal stage-driven
401 transcriptional patterns may relate to differential light adaptation in populations originating in
402 offshore versus nearshore waters. Inshore populations, potentially adapted to life in turbid
403 waters, may increase transcription upon dark enclosure, whereas offshore populations
404 (transported shoreward during flood tide) may be adapted to clearer waters and reduce
405 transcription in dark conditions.

406 Multiple lines of evidence indicate coastal *Ca. Poseidoniales* were metabolizing proteins
407 and fatty acids. High transcription of genes encoding proteases or peptidases mapping to all *Ca.*
408 *Poseidoniales* MAGs (Fig. 2) suggests metabolism of proteins or peptides by both families
409 (Table 1). Furthermore, decreased transcription of protease genes mapping to the O1 MAG
410 during dark incubations (Fig. 5) suggests protein metabolism by *Ca. Thalassarchaeaceae* was
411 active *in situ* prior to incubation. While some of these genes could be involved in intracellular
412 recycling (particularly lon protease and cytosol aminopeptidase), active protein metabolism is
413 consistent with previous experiments demonstrating protein assimilation [10] and high
414 transcription of *Ca. Poseidoniales* peptidase genes in other marine regions [20,21].

415 In addition to genes encoding protein catabolism, high transcription of the 3-
416 hydroxyacyl-CoA dehydrogenase gene from all three MAGs (Fig. 2), and its enrichment in O1-
417 active field samples (Fig. 3), suggests the importance of fatty acid metabolism for both *Ca.*

418 Poseidoniales families (Table 1). This conclusion fits with the widespread occurrence of β -
419 oxidation genes in *Ca. Poseidoniales* MAGs [15,16], as well as transcriptional data from the
420 deep ocean [21].

421

422 DISTINCT PATTERNS OF AMINO ACID AND NUCLEOTIDE UPTAKE AND 423 METABOLISM

424 Transcription of *livK* and *aapJ* appears to differentiate *Ca. Poseidoniales* families in the
425 coastal ocean (Table 1). These genes putatively encode ligand-binding receptors for ABC
426 transporters: *aapJ* for a general L-amino acid transporter and *livK* for a branched-chain amino
427 acid transporter [92]. Both are commonly present in *Ca. Thalassarchaeaceae* (MGIIb) but not *Ca.*
428 *Poseidoniaceae* (MGIIa) [16] and were among the most highly transcribed *Ca.*
429 *Thalassarchaeaceae* genes (Fig. 2). Previous studies noted high transcription of euryarchaeal *livK*
430 and *aapJ* genes in the water column of the Red Sea [19,20], at the Mid-Cayman Rise [21], and
431 throughout the Atlantic Ocean [22]. Our data suggest this activity was probably associated with
432 *Ca. Thalassarchaeaceae*.

433 The *aapJ* and *livK* genes were collocated with genes putatively encoding the full
434 transporters in the *Ca. Thalassarchaeaceae* MAGs (Table S1). Unfortunately, it is difficult to
435 guess their substrates from sequence data alone: AAP transporters are typically capable of
436 transporting a range of L-amino acids [92] while LIV transporters can be highly specific for
437 leucine, specific for branched-chain amino acids, or transport diverse amino acids [92-94]. In soil
438 bacteria grown under inorganic nitrogen limitation, elevated transcription of *aapJ* is linked to
439 organic nitrogen use [95], but it is unclear whether this mechanism translates to *Ca.*
440 *Thalassarchaeaceae* since amino acids could be used for numerous anabolic or catabolic

441 processes. In addition to these binding proteins, the depletion of transcripts from O1 genes
442 putatively involved in the shikimate pathway of aromatic amino acid synthesis (3-
443 phosphoshikimate 1-carboxyvinyltransferase and anthranilate synthase) during incubations (Fig.
444 5) suggests these archaea were synthesizing aromatic amino acids *in situ*.

445 The combination of high *pbuG* transcription by *Ca. Thalassarchaeaceae* (MGIIb) with the
446 high numbers of O1 *pbuG* transcripts in O1-active samples and dark incubation endpoints (Figs.
447 2,3,5) suggests an important role for xanthine/uracil permease (the putative product of *pbuG*) in
448 *Ca. Thalassarchaeaceae* metabolism. In some phytoplankton, *pbuG* is transcribed during
449 nitrogen-stressed growth [96-98], potentially allowing access to DON. However, *pbuG* and
450 xanthine dehydrogenase (*xdh*) are also transcribed when xanthine is catabolized by marine
451 bacteria [99]. Both *Ca. Thalassarchaeaceae* MAGs contain putative xanthine dehydrogenase
452 genes (*xdhC* and *yagS*; Table S1), suggesting the ability to catabolize xanthine (Table 1).

453 Transcription levels of *carA*, putatively encoding part of carbamoyl phosphate synthetase,
454 appears to be a distinct trait of *Ca. Poseidoniaceae* (MGIIa): while all three MAGs contained this
455 gene (Table S1), only *Ca. Poseidoniaceae carA* transcription was high. Since carbamoyl
456 phosphate synthetase is a key enzyme for arginine and pyrimidine synthesis from bicarbonate,
457 high *carA* transcription suggests these pathways may be important components of *Ca.*

458 *Poseidoniaceae* growth or survival.

459

460 CONCLUSIONS

461 Our metatranscriptomic data and associated experiments provide a window into the
462 activity of *Ca. Poseidoniales* families (formerly “MGIIa” and “MGIIb”). They indicate an
463 important role for *Ca. Thalassarchaeaceae* (MGIIb) as coastal photoheterotrophs, particularly in

464 warm waters. High transcription of proteorhodopsin and membrane-bound pyrophosphatase
465 genes suggested common methods for establishing proton gradients. Furthermore, high
466 transcription of genes involved in protein/peptide metabolism and β -oxidation of fatty acids
467 confirmed peptide and lipid metabolism as a common trait. However, high transcription of *Ca.*
468 *Thalassarchaeaceae* genes encoding amino acid binding proteins and nucleotide transporters
469 suggests uptake of these substrates may distinguish the two families. These data confirm the
470 importance of DOM metabolism by *Ca.* *Poseidoniales* and suggest a potential role for organic
471 nitrogen in *Ca.* *Thalassarchaeaceae* metabolism.

472

473 **ACKNOWLEDGMENTS**

474 We thank Qian Liu, Bradley Tolar, the Georgia Coastal Ecosystems LTER field team, the
475 University of Georgia Marine Institute at Sapelo Island staff, and the captain and crew of the
476 R/V *Savannah* for assistance with original field sampling. This work was funded in part by NSF
477 OCE grant 1538677 and OPP grant 1643466 (to JTH), NSF Grant IOS1656311 (to MAM), and
478 NSF OCE grant 1832178 (to the Georgia Coastal Ecosystems LTER), as well as by resources
479 and technical expertise from the Georgia Advanced Computing Resource Center, a partnership
480 between the University of Georgia's Office of the Vice President for Research and Office of the
481 Vice President for Information Technology.

482 The authors declare no competing financial interests.

483 **REFERENCES**

- 484 1. Fuhrman JA, McCallum K, Davis AA. Novel major archaeobacterial group from marine plankton. *Nature*
485 1992;356:148–9.
- 486 2. DeLong EF. Archaea in coastal marine environments. *Proceedings of the National Academy of Sciences*
487 1992;89:5685–9.
- 488 3. Zhang CL, Xie W, Martín-Cuadrado A-B, Rodriguez-Valera F. Marine Group II Archaea, potentially
489 important players in the global ocean carbon cycle. *Frontiers in Microbiology* 2015;6:1108.
- 490 4. Santoro AE, Richter RA, Dupont CL. Planktonic marine archaea. *Annual Review of Marine Science*
491 2019;11:131–58.

- 492 5. Bèjà O, Suzuki MT, Koonin EV, Aravind L, Hadd A, Nguyen LP, et al. Construction and analysis of
493 bacterial artificial chromosome libraries from a marine microbial assemblage. *Environmental*
494 *Microbiology* 2000;2:516–29.
- 495 6. Moreira D, Rodriguez-Valera F, López-García P. Analysis of a genome fragment of a deep-sea
496 uncultivated Group II euryarchaeote containing 16S rDNA, a spectinomycin-like operon and several
497 energy metabolism genes. *Environmental Microbiology* 2004;6:959–69.
- 498 7. Martín-Cuadrado A-B, Rodriguez-Valera F, Moreira D, Alba JC, Ivars-Martínez E, Henn MR, et al.
499 Hindsight in the relative abundance, metabolic potential and genome dynamics of uncultivated marine
500 archaea from comparative metagenomic analyses of bathypelagic plankton of different oceanic regions.
501 *The ISME Journal* 2008;2:865–86.
- 502 8. Alonso C, Pernthaler J. Concentration-dependent patterns of leucine incorporation by coastal
503 picoplankton. *Applied and Environmental Microbiology* 2006;72:2141–7.
- 504 9. Orsi WD, Smith JM, Wilcox HM, Swalwell JE, Carini P, Worden AZ, et al. Ecophysiology of
505 uncultivated marine euryarchaea is linked to particulate organic matter. *The ISME Journal* 2015;9:1747–
506 63.
- 507 10. Orsi WD, Smith JM, Liu S, Liu Z, Sakamoto CM, Wilken S, et al. Diverse, uncultivated bacteria and
508 archaea underlying the cycling of dissolved protein in the ocean. *The ISME Journal* 2016;10:2158–73.
- 509 11. Iverson V, Morris RM, Frazar CD, Berthiaume CT, Morales RL, Armbrust EV. Untangling genomes from
510 metagenomes: revealing an uncultured class of marine *Euryarchaeota*. *Science* 2012;335:587–90.
- 511 12. Martín-Cuadrado A-B, Garcia-Heredia I, Gonzaga Moltó A, López-Ubeda R, Kimes N, López-García P,
512 et al. A new class of marine Euryarchaeota group II from the mediterranean deep chlorophyll maximum.
513 *The ISME Journal* 2015;9:1619–34.
- 514 13. Thrash JC, Seitz KW, Baker BJ, Temperton B, Gillies LE, Rabalais NN, et al. Metabolic roles of
515 uncultivated bacterioplankton lineages in the northern Gulf of Mexico “dead zone.” *mBio* 2017;8:e01017–
516 17.
- 517 14. Orellana LH, Francis TB, Krüger K, Teeling H, Müller M-C, Fuchs BM, et al. Niche differentiation
518 among annually recurrent coastal Marine Group II Euryarchaeota. *The ISME Journal* 2019;13:3024–36.
- 519 15. Rinke C, Rubino F, Messer LF, Youssef N, Parks DH, Chuvochina M, et al. A phylogenomic and
520 ecological analysis of the globally abundant Marine Group II archaea (*Ca. Poseidoniales* ord. nov.). *The*
521 *ISME Journal* 2019;13:663–75.
- 522 16. Tully BJ. Metabolic diversity within the globally abundant Marine Group II Euryarchaea offers insight
523 into ecological patterns. *Nature Communications* 2019;10:271.
- 524 17. Baker BJ, Sheik CS, Taylor CA, Jain S, Bhasi A, Cavalcoli JD, et al. Community transcriptomic assembly
525 reveals microbes that contribute to deep-sea carbon and nitrogen cycling. *The ISME Journal* 2013;7:1962–
526 73.
- 527 18. Ottesen EA, Young CR, Gifford SM, Eppley JM, Marin R, Schuster SC, et al. Multispecies diel
528 transcriptional oscillations in open ocean heterotrophic bacterial assemblages. *Science* 2014;345:207–12.
- 529 19. Miller D, Pfreundt U, Hou S, Lott SC, Hess WR, Berman-Frank I. Winter mixing impacts gene expression
530 in marine microbial populations in the Gulf of Aqaba. *Aquatic Microbial Ecology* 2017;80:223–42.
- 531 20. Hou S, Pfreundt U, Miller D, Berman-Frank I, Hess WR. mdRNA-Seq analysis of marine microbial
532 communities from the northern Red Sea. *Scientific Reports* 2016;6:35470.
- 533 21. Li M, Baker BJ, Anantharaman K, Jain S, Breier JA, Dick GJ. Genomic and transcriptomic evidence for
534 scavenging of diverse organic compounds by widespread deep-sea archaea. *Nature Communications*
535 2015;6:8933.
- 536 22. Bergauer K, Fernandez-Guerra A, Garcia JAL, Sprenger RR, Stepanauskas R, Pachiadaki MG, et al.
537 Organic matter processing by microbial communities throughout the Atlantic water column as revealed by
538 metaproteomics. *Proceedings of the National Academy of Sciences* 2018;115:E400–8.
- 539 23. Vorobev A, Sharma S, Yu M, Lee J, Washington BJ, Whitman WB, et al. Identifying labile DOM
540 components in a coastal ocean through depleted bacterial transcripts and chemical signals. *Environmental*
541 *Microbiology* 2018;20:3012–30.

- 542 24. Liu Q, Tolar BB, Ross MJ, Cheek JB, Sweeney CM, Wallsgrove NJ, et al. Light and temperature control
543 the seasonal distribution of thaumarchaeota in the South Atlantic bight. *The ISME Journal* 2018;12:1473–
544 85.
- 545 25. Damashek J, Edwardson CF, Tolar BB, Gifford SM, Moran MA, Hollibaugh JT. Coastal ocean
546 metagenomes and curated metagenome-assembled genomes from Marsh Landing, Sapelo Island (Georgia,
547 USA). *Microbiology Resource Announcements* 2019;8:e00934–19.
- 548 26. Gifford SM, Sharma S, Moran MA. Linking activity and function to ecosystem dynamics in a coastal
549 bacterioplankton community. *Frontiers in Microbiology* 2014;5:185.
- 550 27. Jain C, Rodriguez-R LM, Phillippy AM, Konstantinidis KT, Aluru S. High throughput ANI analysis of
551 90K prokaryotic genomes reveals clear species boundaries. *Nature Communications* 2018;9:5114.
- 552 28. Hug LA, Baker BJ, Anantharaman K, Brown CT, Probst AJ, Castelle CJ, et al. A new view of the tree of
553 life. *Nature Microbiology* 2016;1:16048.
- 554 29. Eren AM, Esen ÖC, Quince C, Vineis JH, Morrison HG, Sogin ML, et al. Anvi'o: an advanced analysis
555 and visualization platform for 'omics data. *PeerJ* 2015;3:e1319.
- 556 30. Eddy SR. Accelerated profile HMM searches. *PLoS Computational Biology* 2011;7:e1002195.
- 557 31. Edgar RC. MUSCLE: multiple sequence alignment with high accuracy and high throughput. *Nucleic
558 Acids Research* 2004;32:1792–7.
- 559 32. Price MN, Dehal PS, Arkin AP. FastTree 2 – approximately maximum-likelihood trees for large
560 alignments. *PLoS ONE* 2010;5:e9490.
- 561 33. Santoro AE, Dupont CL, Richter RA, Craig MT, Carini P, McIlvin MR, et al. Genomic and proteomic
562 characterization of “*Candidatus Nitrosopelagicus brevis*”: An ammonia-oxidizing archaeon from the open
563 ocean. *Proceedings of the National Academy of Sciences* 2015;112:1173–8.
- 564 34. Langmead B, Salzberg SL. Fast gapped-read alignment with Bowtie 2. *Nature Methods* 2012;9:357–9.
- 565 35. Li H, Handsaker B, Wysoker A, Fennell T, Ruan J, Homer N, et al. The Sequence Alignment/Map format
566 and SAMtools. *Bioinformatics* 2009;25:2078–9.
- 567 36. Satinsky BM, Gifford SM, Crump BC, Moran MA. Use of Internal Standards for Quantitative
568 Metatranscriptome and Metagenome Analysis. In: DeLong EF, editor. *Methods in Enzymology Microbial
569 Metagenomics, Metatranscriptomics, and Metaproteomics*. Elsevier Inc; 2013. pages 237–50.
- 570 37. R Core Team. R: A language and environment for statistical computing. R Foundation for Statistical
571 Computing, Vienna, Austria. <https://www.R-project.org/>. 2019;
- 572 38. de Mendiburu F. agricolae: Statistical procedures for agricultural research. R package version 1.3-1.
573 <https://CRAN.R-project.org/package=agricolae>. 2019;
- 574 39. Oksanen J, Blanchet FG, Friendly M, Kindt R, Legendre P, McGlenn D, et al. vegan: Community ecology
575 package. R package version 2.5-5. <https://CRAN.R-project.org/package=vegan>. 2019;
- 576 40. Legendre P, Legendre L. *Numerical Ecology*. 3rd ed. Elsevier; 2012.
- 577 41. Tully BJ, Graham ED, Heidelberg JF. The reconstruction of 2,631 draft metagenome-assembled genomes
578 from the global oceans. *Scientific Data* 2018;5:170103.
- 579 42. Sunagawa S, Coelho LP, Chaffron S, Kultima JR, Labadie K, Salazar G, et al. Structure and function of
580 the global ocean microbiome. *Science* 2015;348:1261359.
- 581 43. Seemann T. Prokka: rapid prokaryotic genome annotation. *Bioinformatics* 2014;30:2068–9.
- 582 44. Buchfink B, Xie C, Huson DH. Fast and sensitive protein alignment using DIAMOND. *Nature Methods*
583 2014;12:59–60.
- 584 45. Huerta-Cepas J, Szklarczyk D, Forslund K, Cook H, Heller D, Walter MC, et al. eggNOG 4.5: a
585 hierarchical orthology framework with improved functional annotations for eukaryotic, prokaryotic and
586 viral sequences. *Nucleic Acids Research* 2016;44:D286–93.
- 587 46. Huerta-Cepas J, Forslund K, Coelho LP, Szklarczyk D, Jensen LJ, Mering von C, et al. Fast genome-wide
588 functional annotation through orthology assignment by eggNOG-mapper. *Molecular Biology and
589 Evolution* 2017;34:2115–22.
- 590 47. Kanehisa M, Sato Y, Morishima K. BlastKOALA and GhostKOALA: KEGG Tools for Functional
591 Characterization of Genome and Metagenome Sequences. *Journal of Molecular Biology* 2016;428:726–
592 31.

- 593 48. Lombard V, Golaconda Ramulu H, Drula E, Coutinho PM, Henrissat B. The carbohydrate-active enzymes
594 database (CAZy) in 2013. *Nucleic Acids Research* 2014;42:D490–5.
- 595 49. Zhang H, Yohe T, Huang L, Entwistle S, Wu P, Yang Z, et al. dbCAN2: a meta server for automated
596 carbohydrate-active enzyme annotation. *Nucleic Acids Research* 2018;46:W95–W101.
- 597 50. Rawlings ND, Barrett AJ, Thomas PD, Huang X, Bateman A, Finn RD. The MEROPS database of
598 proteolytic enzymes, their substrates and inhibitors in 2017 and a comparison with peptidases in the
599 PANTHER database. *Nucleic Acids Research* 2017;46:D624–32.
- 600 51. Saier MH Jr, Reddy VS, Tsu BV, Ahmed MS, Li C, Moreno-Hagelsieb G. The Transporter Classification
601 Database (TCDB): recent advances. *Nucleic Acids Research* 2016;44:D372–9.
- 602 52. Love MI, Huber W, Anders S. Moderated estimation of fold change and dispersion for RNA-seq data with
603 DESeq2. *Genome Biology* 2014;15:550.
- 604 53. Damashek J, Tolar BB, Liu Q, Okotie Oyekan AO, Wallsgrove NJ, Popp BN, et al. Microbial oxidation of
605 nitrogen supplied as selected organic nitrogen compounds in the South Atlantic Bight. *Limnology and
606 Oceanography* 2019;64:982–95.
- 607 54. Massana R, Murray AE, Preston CM, DeLong EF. Vertical distribution and phylogenetic characterization
608 of marine planktonic *Archaea* in the Santa Barbara Channel. *Applied and Environmental Microbiology*
609 1997;63:50–6.
- 610 55. Teira E, Reinthaler T, Pernthaler A, Pernthaler J, Herndl GJ. Combining catalyzed reporter deposition-
611 fluorescence in situ hybridization and microautoradiography to detect substrate utilization by bacteria and
612 archaea in the deep ocean. *Applied and Environmental Microbiology* 2004;70:4411–4.
- 613 56. Galand PE, Gutiérrez-Provecho C, Massana R, Gasol JM, Casamayor EO. Inter-annual recurrence of
614 archaeal assemblages in the coastal NW Mediterranean Sea (Blanes Bay Microbial Observatory).
615 *Limnology and Oceanography* 2010;55:2117–25.
- 616 57. Legendre P. lmodel2: Model II regression. R package version 1.7-3.
617 <https://CRAN.R-project.org/package=lmodel2>. 2018;
- 618 58. Wickham H. ggplot2: Elegant Graphics for Data Analysis. New York: Springer; 2016.
- 619 59. Man D, Wang W, Sabeji G, Aravind L, Post AF, Massana R, et al. Diversification and spectral tuning in
620 marine proteorhodopsins. *The EMBO Journal* 2003;22:1725–31.
- 621 60. Gómez-Consarnau L, González JM, Coll-Lladó M, Gourdon P, Pascher T, Neutze R, et al. Light
622 stimulates growth of proteorhodopsin-containing marine Flavobacteria. *Nature* 2007;445:210–3.
- 623 61. Pinhassi J, DeLong EF, Beja O, González JM, Pedrós-Alio C. Marine bacterial and archaeal ion-pumping
624 rhodopsins: genetic diversity, physiology, and ecology. *Microbiology and Molecular Biology Reviews*
625 2016;80:929–54.
- 626 62. Church MJ, DeLong EF, Ducklow HW, Karner MB, Preston CM, Karl DM. Abundance and distribution
627 of planktonic Archaea and Bacteria in the waters west of the Antarctic Peninsula. *Limnology and
628 Oceanography* 2003;48:1893–902.
- 629 63. Herndl GJ, Reinthaler T, Teira E, van Aken H, Veth C, Pernthaler A, et al. Contribution of *Archaea* to
630 total prokaryotic production in the deep Atlantic Ocean. *Applied and Environmental Microbiology*
631 2005;71:2303–9.
- 632 64. Galand PE, Lovejoy C, Hamilton AK, Ingram RG, Pedneault E, Carmack EC. Archaeal diversity and a
633 gene for ammonia oxidation are coupled to oceanic circulation. *Environmental Microbiology*
634 2009;11:971–80.
- 635 65. Lincoln SA, Wai B, Eppley JM, Church MJ, Summons RE, DeLong EF. Planktonic Euryarchaeota are a
636 significant source of archaeal tetraether lipids in the ocean. *Proceedings of the National Academy of
637 Sciences* 2014;111:9858–63.
- 638 66. Liu H, Zhang CL, Yang C, Chen S, Cao Z, Zhang Z, et al. Marine Group II dominates planktonic archaea
639 in water column of the northeastern South China Sea. *Frontiers in Microbiology* 2017;8:1098.
- 640 67. Mincer TJ, Church MJ, Taylor LT, Preston C, Karl DM, DeLong EF. Quantitative distribution of
641 presumptive archaeal and bacterial nitrifiers in Monterey Bay and the North Pacific Subtropical Gyre.
642 *Environmental Microbiology* 2007;9:1162–75.

- 643 68. Stoica E, Herndl GJ. Contribution of *Crenarchaeota* and *Euryarchaeota* to the prokaryotic plankton in the
644 coastal northwestern Black Sea. *Journal of Plankton Research* 2007;29:699–706.
- 645 69. Xie W, Luo H, Murugapiran SK, Dodsworth JA, Chen S, Sun Y, et al. Localized high abundance of
646 Marine Group II archaea in the subtropical Pearl River Estuary: implications for their niche adaptation.
647 *Environmental Microbiology* 2018;20:734–54.
- 648 70. Wang ZA, Cai W-J, Wang Y, Ji H. The southeastern continental shelf of the United States as an
649 atmospheric CO₂ source and an exporter of inorganic carbon to the ocean. *Continental Shelf Research*
650 2005;25:1917–41.
- 651 71. Letourneau ML, Medeiros PM. Dissolved organic matter composition in a marsh-dominated estuary:
652 response to seasonal forcing and to the passage of a hurricane. *Journal of Geophysical Research:*
653 *Biogeosciences* 2019;124:1545–59.
- 654 72. Medeiros PM, Babcock Adams L, Seidel M, Castelao RM, Di Iorio D, Hollibaugh JT, et al. Export of
655 terrigenous dissolved organic matter in a broad continental shelf. *Limnology and Oceanography*
656 2017;62:1718–31.
- 657 73. Herfort L, Schouten S, Abbas B, Veldhuis MJW, Coolen MJL, Wuchter C, et al. Variations in spatial and
658 temporal distribution of Archaea in the North Sea in relation to environmental variables. *FEMS*
659 *Microbiology Ecology* 2007;62:242–57.
- 660 74. Hugoni M, Taib N, Debroas D, Domaizon I, Jouan Dufournel I, Bronner G, et al. Structure of the rare
661 archaeal biosphere and seasonal dynamics of active ecotypes in surface coastal waters. *Proceedings of the*
662 *National Academy of Sciences* 2013;110:6004–9.
- 663 75. Bano N, Ruffin S, Ransom B, Hollibaugh JT. Phylogenetic composition of Arctic Ocean archaeal
664 assemblages and comparison with Antarctic assemblages. *Applied and Environmental Microbiology*
665 2004;70:781–9.
- 666 76. Parada AE, Fuhrman JA. Marine archaeal dynamics and interactions with the microbial community over 5
667 years from surface to seafloor. *The ISME Journal* 2017;11:2510–25.
- 668 77. Pereira O, Hochart C, Auguet J-C, Debroas D, Galand PE. Genomic ecology of Marine Group II, the most
669 common marine planktonic Archaea across the surface ocean. *MicrobiologyOpen* 2019;8:e852.
- 670 78. Bèjà O, Aravind L, Koonin EV, Suzuki MT, Hadd A, Nguyen LP, et al. Bacterial rhodopsin: evidence for
671 a new type of phototrophy in the sea. *Science* 2000;289:1902–6.
- 672 79. Frias-Lopez J, Shi Y, Tyson GW, Coleman ML, Schuster SC, Chisholm SW, et al. Microbial community
673 gene expression in ocean surface waters. *Proceedings of the National Academy of Sciences*
674 2008;105:3805–10.
- 675 80. Poretsky RS, Hewson I, Sun S, Allen AE, Zehr JP, Moran MA. Comparative day/night metatranscriptomic
676 analysis of microbial communities in the North Pacific subtropical gyre. *Environmental Microbiology*
677 2009;11:1358–75.
- 678 81. Satinsky BM, Crump BC, Smith CB, Sharma S, Zielinski BL, Doherty M, et al. Microspatial gene
679 expression patterns in the Amazon River Plume. *Proceedings of the National Academy of Sciences*
680 2014;111:11085–90.
- 681 82. Alonso-Sáez L, Morán XAG, González JM. Transcriptional patterns of biogeochemically relevant marker
682 genes by temperate marine bacteria. *Frontiers in Microbiology* 2020;11:465.
- 683 83. Arandia-Gorostidi N, González JM, Huete-Stauffer T, Ansari MI, Morán XAG, Alonso-Sáez L. Light
684 supports cell-integrity and growth rates of taxonomically diverse coastal photoheterotrophs.
685 *Environmental Microbiology* 2020;
- 686 84. Giovannoni SJ, Bibbs L, Cho J-C, Stapels MD, Desiderio R, Vergin KL, et al. Proteorhodopsin in the
687 ubiquitous marine bacterium SAR11. *Nature* 2005;438:82–5.
- 688 85. Kimura H, Young CR, Martinez A, DeLong EF. Light-induced transcriptional responses associated with
689 proteorhodopsin-enhanced growth in a marine flavobacterium. *The ISME Journal* 2011;5:1641–51.
- 690 86. Steindler L, Schwalbach MS, Smith DP, Chan F, Giovannoni SJ. Energy starved *Candidatus Pelagibacter*
691 ubique substitutes light-mediated ATP production for endogenous carbon respiration. *PLoS ONE*
692 2011;6:e19725.

- 693 87. Song Y, Cartron ML, Jackson PJ, Davison PA, Dickman MJ, Zhu D, et al. Proteorhodopsin
694 overproduction enhances the long-term viability of *Escherichia coli*. Applied and Environmental
695 Microbiology 2020;86:e02087–19.
- 696 88. Baykov AA, Malinen AM, Luoto HH, Lahti R. Pyrophosphate-fueled Na⁺ and H⁺ transport in
697 prokaryotes. Microbiology and Molecular Biology Reviews 2013;77:267–76.
- 698 89. Rinta-Kanto JM, Sun S, Sharma S, Kiene RP, Moran MA. Bacterial community transcription patterns
699 during a marine phytoplankton bloom. Environmental Microbiology 2012;14:228–39.
- 700 90. Vila-Costa M, Sharma S, Moran MA, Casamayor EO. Diel gene expression profiles of a phosphorus
701 limited mountain lake using metatranscriptomics. Environmental Microbiology 2013;15:1190–203.
- 702 91. Needham DM, Fuhrman JA. Pronounced daily succession of phytoplankton, archaea and bacteria
703 following a spring bloom. Nature Microbiology 2016;1:16005.
- 704 92. Hosie AHF, Poole PS. Bacterial ABC transporters of amino acids. Research in Microbiology
705 2001;152:259–70.
- 706 93. Anderson JJ, Oxender DL. *Escherichia coli* transport mutants lacking binding protein and other
707 components of the branched-chain amino acid transport systems. Journal of Bacteriology 1977;130:384–
708 92.
- 709 94. Montesinos ML, Herrero A, Flores E. Amino acid transport in taxonomically diverse cyanobacteria and
710 identification of two genes encoding elements of a neutral amino acid permease putatively involved in
711 recapture of leaked hydrophobic amino acids. Journal of Bacteriology 1997;179:853–62.
- 712 95. Walshaw DL, Reid CJ, Poole PS. The general amino acid permease of *Rhizobium leguminosarum* strain
713 3841 is negatively regulated by the Ntr system. FEMS Microbiology Letters 1997;152:57–64.
- 714 96. Berg GM, Shrager J, Glöckner G, Arrigo KR, Grossman AR. Understanding nitrogen limitation in
715 *Aureococcus anophagefferens* (Pelagophyceae) through cDNA and qRT-PCR analysis. Journal of
716 Phycology 2008;44:1235–49.
- 717 97. Wurch LL, Gobler CJ, Dyhrman ST. Expression of a xanthine permease and phosphate transporter in
718 cultures and field populations of the harmful alga *Aureococcus anophagefferens*: tracking nutritional
719 deficiency during brown tides. Environmental Microbiology 2014;16:2444–57.
- 720 98. Cooper JT, Sinclair GA, Wawrik B. Transcriptome analysis of *Scrippsiella trochoidea* CCMP 3099
721 reveals physiological changes related to nitrate depletion. Frontiers in Microbiology 2016;7:639.
- 722 99. Cunliffe M. Purine catabolic pathway revealed by transcriptomics in the model marine bacterium
723 *Ruegeria pomeroyi* DSS-3. FEMS Microbiology Ecology 2016;92:fiv150.
- 724